RELATION BETWEEN RAYLEIGH WAVES AND UPLIFT OF THE SEABED FOR RAPID TSUNAMI DETECTION

S. Inoue[1)], T. Ohmachi[2)]

1) Research Associate, Department of Built Environment, Tokyo Institute of Technology, Japan
2) Professor, Department of Built Environment, Tokyo Institute of Technology, Japan
shusaku@enveng.titech.ac.jp, ohmachi@enveng.titech.ac.jp

Abstract: In recent years, serious damages have been caused by near field tsunamis whose arrival time is less than or equal to a few minutes after the occurrence of earthquakes. In this research, to develop a new tsunami warning system that is more quickly and more accurate than the current systems, we aimed Rayleigh wave inducng the sea surface disturbance preceding tsunami. For this purpose, we research the characteristics of Rayleigh wave and the sea surface disturbance from simulation and real data. The good correlation between the static uplift and the displacement of Rayleigh waves was found on the hanging wall side of the fault plane only.

1. INTRODUCTION

In recent years, serious damages have been caused by near field tsunamis whose arrival time is less than or equal to a few minutes after the occurrence of earthquakes. Current tsunami warning systems need at least some minutes to announce tsunami warning because they are usually based on submarine faults estimated from seismic data observed at several points. Additionally, the wave height estimated from the real time tsunami warning system does not correspond to the actual wave height in near field owing to some approximations in that estimation.

To develop a new tsunami warning system that is more quickly and more accurate than the current systems, we are trying to make use of Rayleigh wave that induces the sea surface disturbance preceding tsunami. The purpose of this study is to investigate the possibility of a tsunami warning system by means of Rayleigh wave and the sea surface disturbance. For this purpose, we study the characteristics of Rayleigh wave and the sea surface disturbance from simulation and real data.

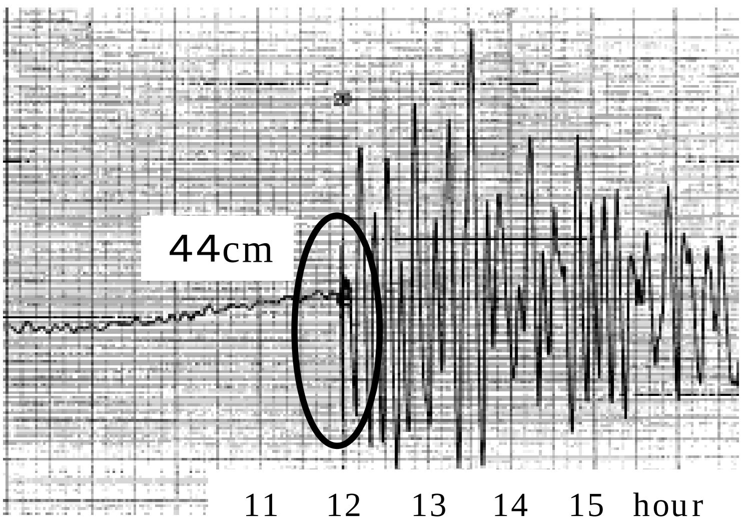

Fig. 1. Tidal record at Fukaura

Figure 1 shows the wave height observed at Fukaura in 1983 Nihonkai-Chubu earthquake. The main purpose of this instrument is to record the tide, so the chart speed is very slow. Each thick line crossing the horizontal axis indicates 1 hour. From this record, long period waves arriving after 12 o'clock can be seen. These waves are the tsunamis that attacked Fukaura. Another wave with amplitude 44cm can be seen at just 12 o'clock, which arrived 7 minutes before the tsunami. This wave is the sea surface disturbance preceding tsunami.

2. TWO-DIMENSIONAL TSUNAMI SIMULATION

The generation of the sea surface disturbance and the tsunami are evaluated by a 2-dimensional simulation. The technique in this simulation is different from conventional ones that use the static seabed displacement and long wave approximation. In the present technique, a total system consisting of the sea water and the underlying ground is assumed to be a weakly coupled system. As a simulation procedure, earthquake ground motion due to seismic fault rupturing is first simulated by the boundary element method (BEM). Then, sea water disturbance including tsunami resulting from the seismic ground motion is simulated by the finite difference method (FDM) using the ground motion velocity as an input to the sea water. In the fluid domain simulation, the governing equation is the Navier-Stokes equation, which accounts for acoustic effects (Ohmachi et al., 2001).

Figure 2 illustrates the analytical model employed. Due to its contribution to tsunami generation we assumed thrust faulting for a 30km wide segment, dipping at 30 degrees, located 7km under the seabed. This fault undergoes unilateral faulting, which means that the fault rupture starts at the bottom of the fault and propagates upward. The rupture velocity, dislocation, and rise time are as shown in Fig. 2. The water depth above the seabed is 3km, and the simulation area extends to +/-100km from the fault.

Snapshots at several seconds after the fault rupturing are shown in Fig 3. The lower and upper surfaces represent the seabed and the sea surface, respectively. At 15sec after the fault rupturing occurs, the wave height in the near-fault area is larger than the seabed displacement. From 20 to 30 sec, Rayleigh waves are generated in the near-fault area, propagating along the seabed, to the right of the figure. The short period sea surface waves travel with the same speed as these Rayleigh waves. The profile of tsunami remaining in the near-fault area at 50 sec propagates to the both side. From this simulation, the sea surface disturbance excited by Rayleigh wave preceding tsunami can be estimated.

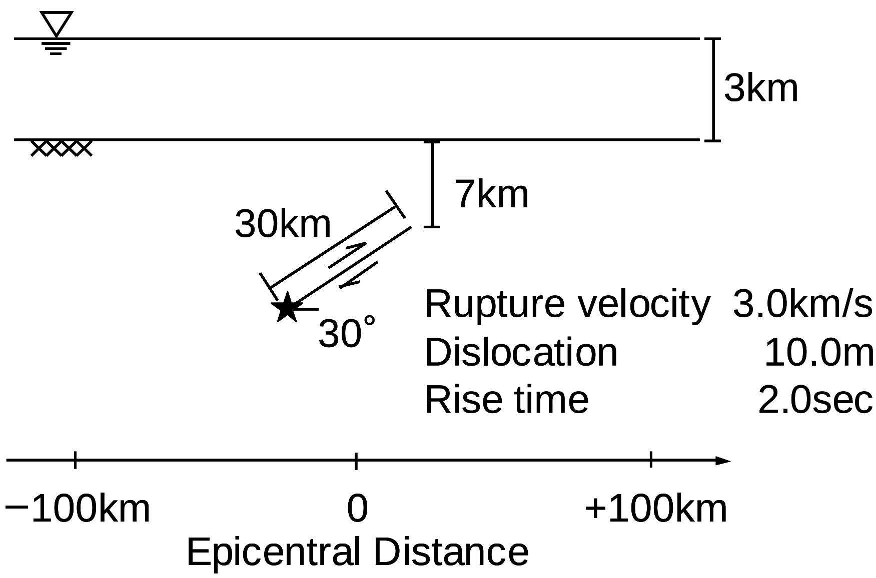

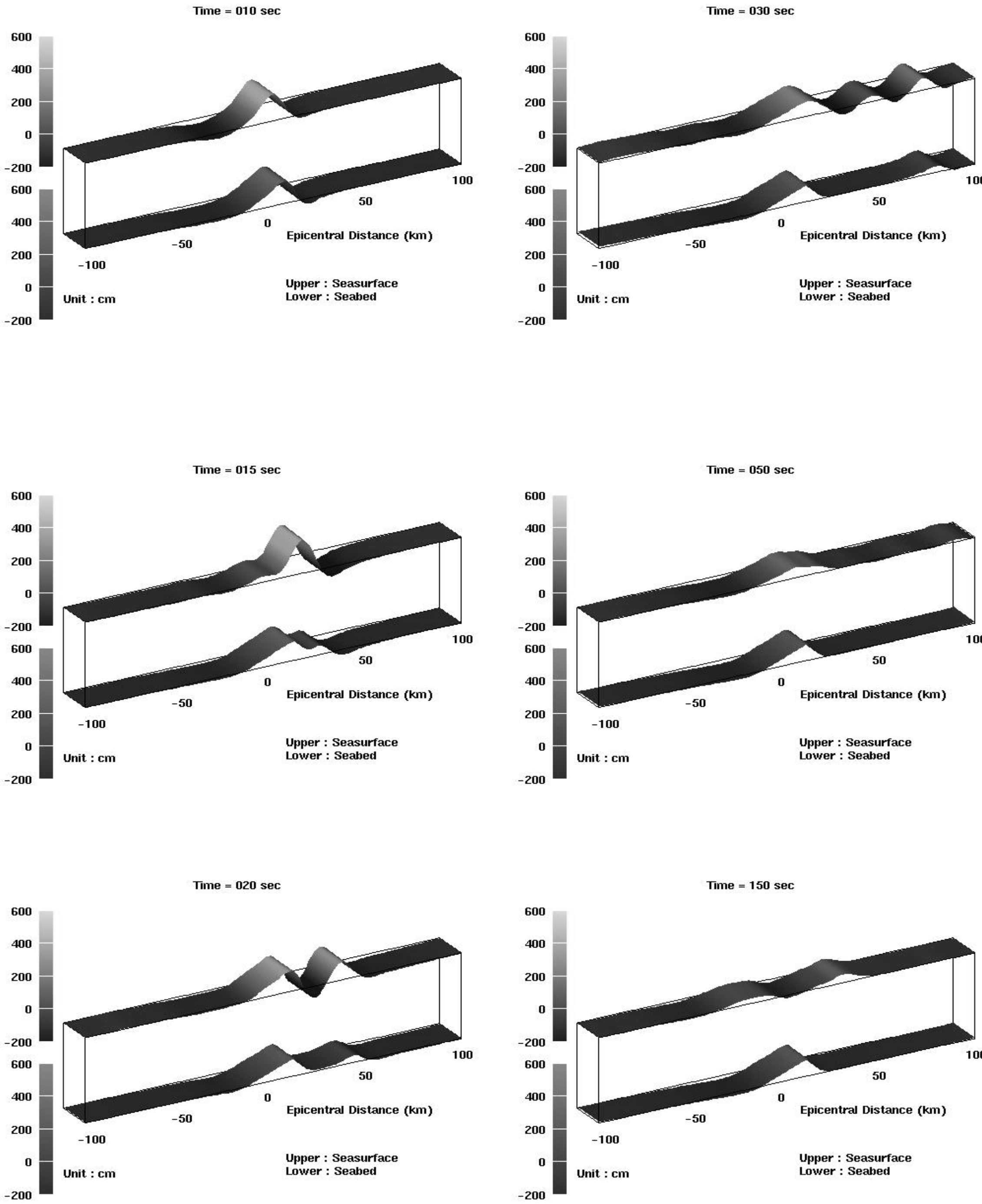

Fig. 3. Two-dimensional tsunami simulation.

3. CHARACTERISTICS OF PROPAGATION

3.1 The 1993 Hokkaido-Nansei-Oki tsunami

To develop a single-point observation system, it is needed to know how Rayleigh waves as well as the sea disturbance propagate from the source area. To investigate the characteristic of the propagation, we check the tidal records of the 1993 Hokkaido-Nansei-Oki tsunami, and the seismic data of the 1999 Chi-Chi Taiwan earthquake.

Figure 4 shows wave height distribution of sea surface disturbance observed prior to the tsunami 1993 Hokaido-Nansei-Oki earthquake. In this figure, tidal observation points and wave height in cm are shown by black circles and numbers. A fault model proposed by Mendoza and Fukuyama(1996) has northern and southern faults. The fault projection is also shown in Fig. 4. In this model, fault rupturing starts at northern fault and propagates to the southern fault. Black stars in Fig. 4 are epicenters of the faults. From the figure, the sea surface disturbances are observed at limited points from Iwanai to Noshiro. These points extend to the south. It is because the sea surface disturbance are induced by Rayleigh waves, which becomes larger gradually as fault rupturing propagates from Northern fault to Southern fault. The Rayleigh wave propagates in the ground, so the sea surface disturbance is observed at Mori where tsunami did not arrive.

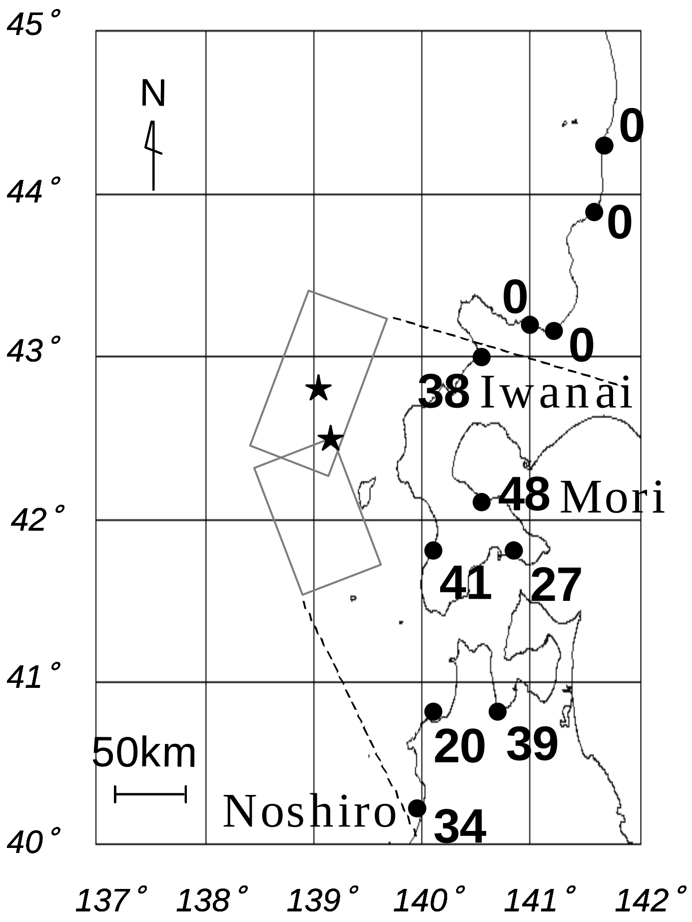

3.2 The 1999 Chi-Chi Taiwan earthquake

The 1999 Chi-Chi Taiwan earthquake is due to low angle thrust-faulting with Ms = 7.6 (USGS), occurred in central Taiwan on September 20, 1999. Though thrust-faulting subduction earthquake causes tsunami frequently, for this reason, we use this earthquake in this study.

Digital seismic acceleration data that contains 441 points all around Taiwan were provided by Lee et al (2001). Figure 5 shows these observation stations and the fault projection proposed by Kikuchi at el. (2000). This fault model is low angle thrust faulting, and slopes down to the east. To find displacement by Rayleigh waves, the vertical acceleration records were integrated with a bandpass filter from 2 to 20 sec.

The distribution of maximum displacement is shown in Fig. 6. From this figure, the displacement is larger on the northwest side of the fault than the other side. Moreover larger displacement is limited to the front of the fault. The epicenter of this earthquake is located at around the center of this fault. We thought that the Rayleigh wave increased in the amplitude gradually on the west side as fault rupturing propagates in shallow area, while the Rayleigh wave does not increased on the east side that fault rupturing propagated in deep area. From the result, it can be thought the Rayleigh wave showed directionality that the amplitude increased in the direction of fault rupturing and in the front area of the fault.

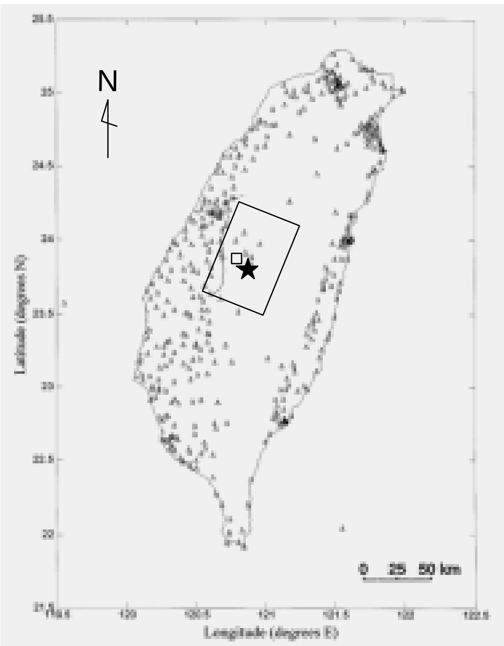

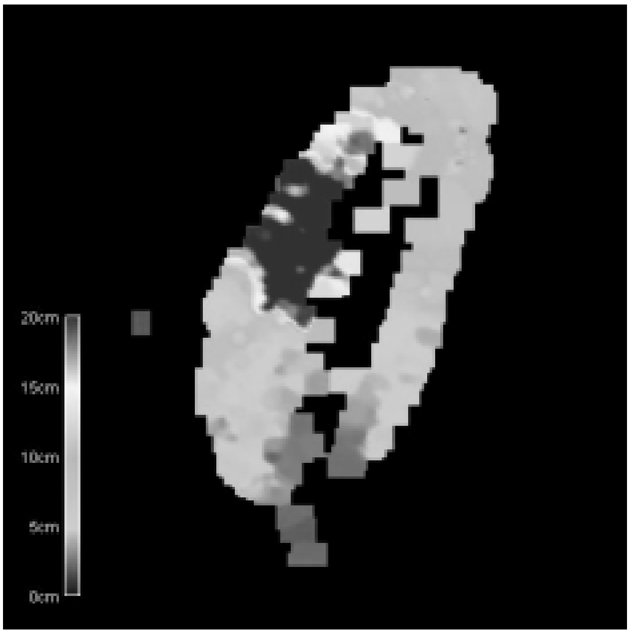

3. CORRELATION BETWEEN THE AMPLITUDE OF GROUND MOTION AND VOLUME OF SEA-BED UPLIFT

To investigate possibility of tsunami warning by means of Rayleigh waves and the sea surface disturbance, next we investigate the relationship between the coseismic ground displacement and the volume of the seabed uplift. First, we define the dynamic maximum displacement and volume of the uplift as shown in Fig. 7. The Volume of the uplift is a part of uplift relative to an observation point (-50km) expressed as a shadow part in the left figure. The dynamic displacement of the ground is the displacement reduced from the maximum displacement to static displacement in Fig. 7.

Figure 8 shows the relationship between the dynamic displacement and the volume in cases of dip angles 30, 45, 60 degree when depth of the fault changes. In the left figure, we can see their correlation looks linear. Similarly, right figure in Fig. 8 shows their relationship when width of the fault changes. The correlation looks almost linear. The linear correlation is found on the hanging wall side in near field area. But, the relation is not linear far field area, or on the foot wall side.

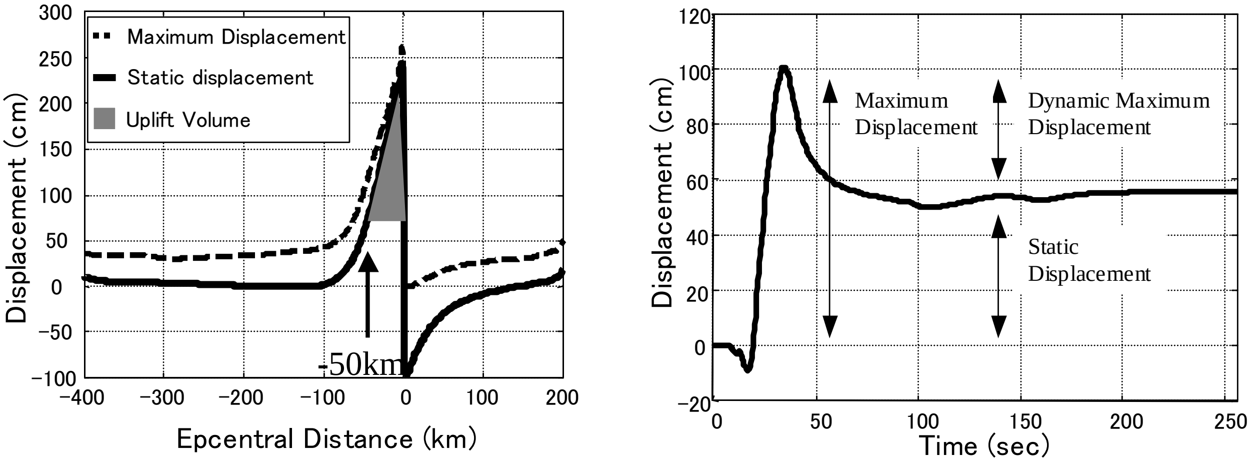

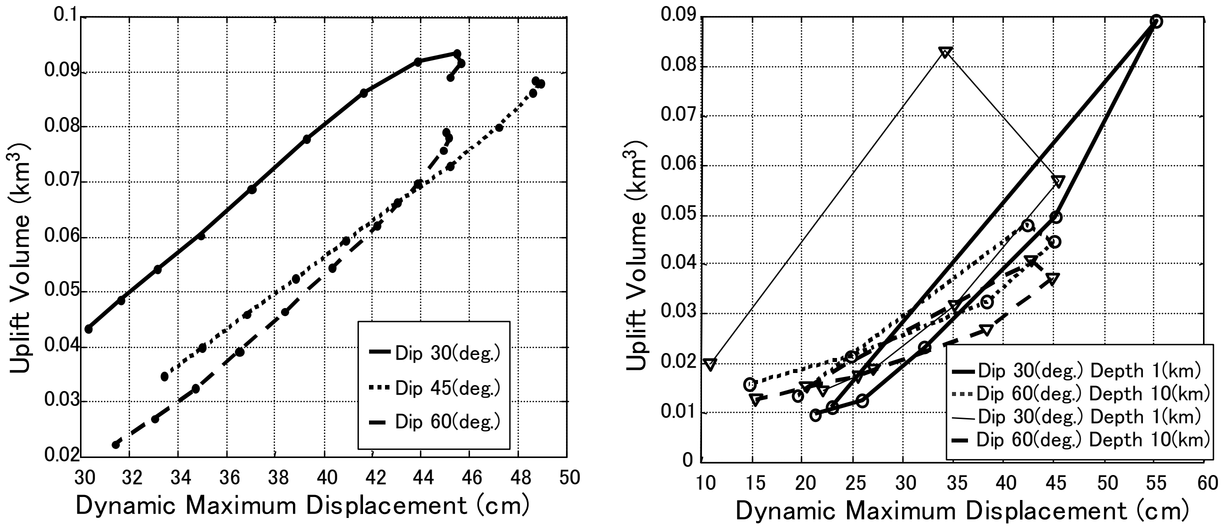

4. CONCLUSIONS

As conclusions, we can point out the followings:

1. Rayleigh waves excite the sea surface disturbance that propagates faster than tsunamis.

2. Rayleigh waves show directionality, from which the amplitude increases in the direction of fault rupturing and in the front area of the fault.

3. A correlation between the dynamic maximum displacement and volume of uplift is almost linear in the near-filed area of hanging wall side.

References:

Ohmachi, T., H. Tsukiyama and H. Matsumoto(2001) : “Simulation of tsunami induced by dynamic displacement of seabed due to seismic faulting”, *Bull. Seism. Soc. Am.*, 91, 6, pp. 1898-1909.

Mendoza, C. and E. Fukuyama(1994) : “The July 1993 Hokkaido-Nansei-Oki, Japan, earthquake : Coseismic slip pattern from strong-motion and teleseismic recordings”, *J. Geophys. Res.*, Vol. 101, pp. 791-801

Lee, W. H. K., T. C. Shin, K. W. Kuo, K. C. Chen and C. F. Wu(2001) : “CWB free-field strong-motion data from the 921 Chi-Chi earthquake” : *processed acceleration files on CD-ROM*, Central Weather Bureu, Taiwan.

Kikuchi, M., Y. Yagi and Y. Yamanaka(2000) : “Source process of the Chi-Chi, Taiwan earthquake of September 21, 1999 inferred from teleseismic body waves”, *Bull. Earthq. Res. Inst.*, Vol. 75, pp. 1-13.